

PASSIVATION STUDY OF Ti_3AlC_2 AND Ti_2AlC IN SELECT ACIDIC SOLUTIONS H_2SO_4 , HCl AND HNO_3

Lylia AOUCHECHE¹, Salem BOUDINAR², Akram ALHUSSEIN³, Mustapha NECHICHE⁴, Said AZEM⁵

In this article, we evaluate the corrosion behavior of the MAX phases Ti_3AlC_2 and Ti_2AlC immersed in selected acidic solutions of 0.36mol H_2SO_4 , HCl or HNO_3 in order to determine the influence of the number of Ti atoms on corrosion resistance. The MAX phases Ti_3AlC_2 and Ti_2AlC were synthesized by hot isostatic pressing (HIP) of Ti -1.9 TiC -Al and Ti -1.2 TiC -Al powders mixture respectively at 1450°C for 2h under argon. The results indicate that Ti_2AlC has better passivation than Ti_3AlC_2 in acidic environments.

The corrosion resistance of Ti_2AlC is mainly due to the rapid formation of a passive film on the surface. Its kinetic corrosion is managed by the dissolution rate of Al and Ti atoms in the acidic solutions. The AAS characterization showed that the Al atoms dissolved from Ti_2AlC in the acidic solution are less than those dissolved from Ti_3AlC_2 . This phenomenon reflects the influence of Ti atoms number on the corrosion resistance in the acid solution used.

Keywords: MAX phases; Ti_3AlC_2 ; Ti_2AlC ; Corrosion behavior; acids; Microstructure

1. Introduction

The MAX phases are layered, hexagonal carbides and nitrides which have the general formula: M_n+1AX_n , (MAX) where $n = 1$ to 3, and M is an early transition metal, A is an A-group (mostly IIIA and IVA, or groups 13 and 14) element and X is either carbon and/or nitrogen. The layered structure consists of edge-sharing, distorted XM_6 octahedra interleaved by single planar layers of the A-group element.

Despite their elaboration for the first time by Jeitschko and al. [1], their popularity returns to Barsoum and al. [2]. These results have motivated the synthesis of MAX phase's materials using different combinations to form ternary carbides or nitrides materials. Their properties are very interesting because they

¹ PhD Student, Mouloud Mammeri University of Tizi-Ouzou, LEC2M Laboratory, Algeria, Corresponding author. E-mail: lylia.aouchiche@ummto.dz

² PhD, Mouloud Mammeri University of Tizi-Ouzou, MPCL Laboratory, Algeria

³ PhD, Technology University of Troyes, LASMIS Laboratory, France

⁴ PhD, Mouloud Mammeri University of Tizi-Ouzou, LEC2M Laboratory, Algeria

⁵ Prof., Mouloud Mammeri University of Tizi-Ouzou, LEC2M Laboratory, Algeria

combine those of metals and ceramics. Thus, they are similar to ceramics by their high temperature rigidity and good corrosion resistance, low coefficient of friction and density and good thermal resistance. In addition, like metals, they have good electrical and thermal conductivity, good machinability, thermal shock resistance, and high strength and rigidity [3-4-5].

Ti_3AlC_2 and Ti_2AlC are extensively studied and are promising candidates for oxidation resistance. These two compounds crystallize in the $P6_3/mmc$ space group and their lattice parameters are respectively ($a = 0.3075$ nm, $c = 1.858$ nm), ($a = 0.304$ nm, $c = 1.360$ nm) [6-7]. Ti_3AlC_2 was first synthesized by Pietzka and Schuster using sintering of a compact mixture of $Ti-C-TiAl-Al_4C_3$ powders. Tzenov and Barsoum also synthesized it by hot isostatic pressing (HIP) at a pressure of 70 MPa and at 1400°C for 16h [8]. Subsequently, there were several studies on the synthesis of Ti_3AlC_2 [9]. Ti_2AlC , firstly it synthesized by hot pressing of $TiC-Al-Ti$ mixture powders at 1400°C but the sintered contains a fine quantity of Ti_3AlC_3 [10]. Zhu also used the hot-pressing method to synthesis it from Ti, Al and C powder smilled by high energy [11]. The spark plasma sintering (SPS) and the reduction via combustion of a $TiO-Mg-Al-C$ mixture are also used for this purpose [12-13].

The electrochemical corrosion behavior, in acid environment, of Ti_3AlC_3 and Ti_2AlC is poorly studied. Travaglini and al studied the corrosion of the Ti_3SiC_2 phase in HCl and H_2SO_4 [14] and also the corrosion behavior of certain MAX phases in NaOH, HCl and H_2SO_4 [15]. Other results cited in references [16] and [17] mentioned that MAX phase containing Ti atoms such as Ti_3AlC_2 , Ti_3SiC_2 and Ti_3GaC_2 presented an excellent oxidation resistance. Dan Li, who has studied the corrosion behavior of Ti_3AlC_2 in H_2SO_4 and NaOH solutions, finds that it has good resistance in NaOH but trans-passivation in H_2SO_4 [18]. The high temperature corrosion resistance of Ti_3AlC_2 has been studied in KOH at 700 °C [19]. The importance of the hexagonal and lamellar structure of Ti_2AlC on corrosion resistance was evaluated in reference [20] and the same result was confirmed using Ti_3SiC_2 immersed in a 3.5% NaCl solution.

In this paper, we studied the corrosion and oxidation behavior of Ti_3AlC_2 and Ti_2AlC in selected acid solutions containing 0.36 moles of H_2SO_4 , HCl or HNO_3 . We revealed the main element behind the difference in corrosion between these two phases. For this, electrochemical (OCP and potentiodynamic polarization) and atomic absorption spectroscopy (AAS) analysis were carried out. The AAS analysis made it possible to identify and quantify the dissolved elements in the acid solutions. In addition, X-ray diffraction (XRD) and scanning electron microscopy (SEM) techniques were used, respectively, for phase identification and observation of surface morphology before and after corrosion.

2. Experimental procedure

2.1 Ti_3AlC_2 and Ti_2AlC and their synthesis

Ti_3AlC_2 and Ti_2AlC are ternary carbides which have interesting properties of both ceramic (refractory, high stiffness, low density) and metal (damage tolerance, thermal shock resistance, high thermal and electrical conductivity). All this gives them a high potential structure and functional material especially in severe environments (high temperature, oxidation, irradiation).

The materials Ti_3AlC_2 and Ti_2AlC , used in this work, were synthesized by HIP sintering, for Ti_3AlC_2 at $1450^\circ C$, for 2 hours under argon, from mixtures of Ti-1.9TiC-Al and for Ti_2AlC at $1500^\circ C$ during 4 hours from Ti-1.2TiC-Al powder mixture.

2.2. *Electrochemical tests and microstructure analysis*

Four samples of similar dimensions (10mm x 10mm x 4mm) were cut from the Ti_3AlC_2 and Ti_2AlC sintered materials. They are then embedded in the resin taking care to put a metal rod in contact with the sample to serve as an electrical conductor. During corrosion tests a surface of 1 cm^2 of MAX phase will be in contact with the electrolyte. This surface is previously polished using alumina suspension and diamond plate up to 0.25 microns and then washed with ethanol in an ultrasonic bath and rinsed with distilled water and finally dried with hot air.

The open circuit potential (OCP) tests were carried out using PGP 201 potentiostat/galvanostat controlled by Power Suite Software. The Potentiodynamic polarization measurements were performed in Autolab PGSTAT-30 potentiostat/galvanostat in a range of ± 300 mV and scan rate of 1mV.s^{-1} , the applied potential was controlled during testing using the GPES 4.9 software. The electrochemical cell was equipped with three electrodes. An Hg/Hg_2Cl_2 electrode is selected as a reference electrode and a platinum mesh as a counter electrode. The electrolytes solutions contain 0.36mol of H_2SO_4 or HCl , HNO_3 . All surface's samples were washed with ethanol before testing and all experiments were repeated four times and carried out at room temperature.

In order to analyze the surface of Ti_3AlC_2 and Ti_2AlC before and after carrying out the potentiodynamic polarization tests, a Philips XL30 scanning electron microscope (SEM) was used and the X-ray diffraction analysis was carried out using the diffractometer BRUKER D8 Advance using $CuK\alpha$ radiation ($\lambda = 1.542\text{ \AA}$). The analyzes were carried out with a 2 mm collimator and an Axial Soller slit with an axial divergence of 2.5° . To identify the corrosion product after the polarization tests, we used razor sharp X-ray diffraction (GAXRD) using a scanning interval of 5° to 90° . The Ti and Al atoms dissolved in the electrolyte

were quantified by atomic absorption spectrometry (AAS) of the SHIMADZU AA-6200 type.

3. Results and discussion

3.1. Open circuit potential

Fig. 1 shows the variation of the corrosion potential (OCP) as a function of the immersion time of Ti_3AlC_2 and Ti_2AlC in acid solutions containing 0.36% mol of H_2SO_4 , HCl or HNO_3 . Data logging started from 5 minutes after immersion with a scan speed of six points per second.

The OCP curves describe the film formation and passivation. In Fig. 1(a, b), we see that just at the beginning of test the potential rapidly shifts towards negative values, proof of the dissolution of the oxide film existing before immersion on both MAX phases [18]. The Ti_2AlC phase was quickly stabilized while some fluctuations were observed for Ti_3AlC_2 phase during tests. In H_2SO_4 , the potential started from -0.28V and decreased to -0.5V. It stabilized for about two hours and then decreased abruptly to -0.64V with little rapid rise to -0.625V. In the HCl solution, the corrosion potential gradually decreased from positive value 0.18V to -0.39V and remains stable for the rest of the time. In both solutions, Ti_3AlC_2 took more time to achieve the potential stabilization.

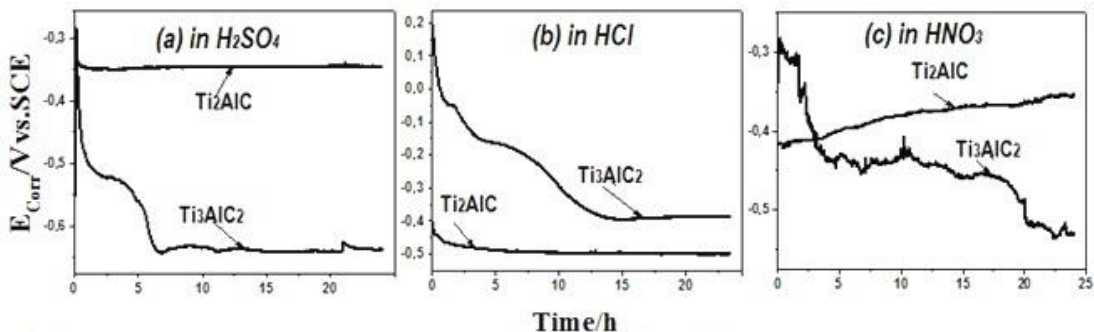


Fig1. Evolution of corrosion potential of Ti_3AlC_2 and Ti_2AlC , for 24 hours, immersed in different acid solutions: a) H_2SO_4 , b) HCl and c) HNO_3 .

In the two acids, H_2SO_4 and HCl , the corrosion potential of Ti_2AlC decreased for a short time from -0.3V to -0.35V and from -0.4V to -0.46V, respectively. For the following time, it remains constant, which means the presence of an intact and resistant film. Contrarily to Ti_3AlC_2 , the potential corrosion took a lot of time and showed some fluctuations before stabilization stage. This means the formation and the dissolution of the protector film made alternatively.

The corrosion potential of Ti_3AlC_2 in HNO_3 (fig1(c)) rapidly decreased from $-0.281V$ to $-0.437V$, and then it stayed constant for some hours showing some fluctuations. From 19h, it decreased again to $-0.533V$ which means the dissolution of Ti_3AlC_2 continuously throughout the test. For Ti_2AlC , is completely different and the corrosion potential of this phase increased during the test. This result indicates the passivation of the Ti_2AlC in HNO_3 due to the formation of an oxide layer on the surface.

3.2. Polarization curves

Potentiodynamic polarization curves of Ti_3AlC_2 and Ti_2AlC in H_2SO_4 , HCl and HNO_3 solutions are given in fig.2. The first measurement was taken at 0h of immersion and the second after 24h. The calculated values of corrosion parameters are presented in tables 1,2 and 3.

In H_2SO_4 and HCl solutions the corrosion potential of Ti_2AlC is lower than that of Ti_3AlC_2 . In H_2SO_4 , at 0h of immersion, Ti_3AlC_2 and Ti_2AlC had corrosion potential of $-0.037V$ and $-0.403V$ and current density of $4.03 \times 10^{-8} A/cm^2$ and $6.51 \times 10^{-6} A/cm^2$, respectively. The anodic part of the polarization curve of Ti_3AlC_2 displayed some perturbations after $-0.009V$ accompanied with a drop in current density, which indicates the beginning of corrosion. Generally, the corrosion's product of Ti_3AlC_2 in H_2SO_4 is mainly sub-oxides of Ti and Al. They don't have enough time to form stable oxides due to the aggressive attack of H^+ [19-20]. After 24h of immersion, the anodic and cathodic parts were smooth and the corrosion potential "Ecorr" reduced contrary to the increasing of current density (table 1).

In HCl solution, at 0h immersion, the anode part indicates that there has been oxidation. At the end of the analysis (after 24h), we observed a decrease in the corrosion current which indicates a pitting corrosion specific to the corrosion behavior of the aluminum alloys.

For both solutions, the Ti_2AlC curves are smooth at 0h of immersion, the oxidation was carried out with H_2SO_4 while a reduction was carried out with a solution of HCl in the presence of H^+ ions. After 24 hours of immersion in both solutions, the two parts of the curves are in equilibrium, indicating that the corrosion occurred in the first hours of immersion.

In HNO_3 , we observed smooth polarization curves for both phases, with the exception of the Ti_3AlC_2 curve at 0h, where some fluctuations are present in the cathodic part. Corrosion in this environment is mainly due to the aggressive H^+ which means that reduction corrosion has occurred in the anode part. We noticed that the current density and potential have increased significantly. The analysis, after 24 hours of immersion, showed an oxidation. All these results confirm the trans-passivation of Ti_3AlC_2 in HNO_3 .

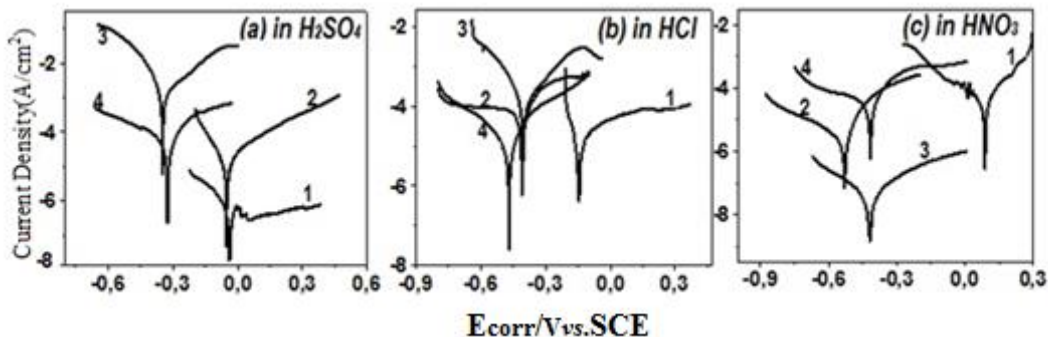


Fig.2. Potentiodynamic polarization curves in acid solutions (H_2SO_4 / HCl / HNO_3); scan rate was 1mV/s. 1) Ti_3AlC_2 at 0h; 2) Ti_2AlC at 0h; 3) Ti_3AlC_2 at 24h; 4) Ti_2AlC at 24h.

For Ti_2AlC , the OCP and polarization curves show that its immersion in HNO_3 makes it more noble material.

Table 1
Electrochemical parameters of MAX phases immersed in H_2SO_4

MAX phases	Immersion Time (h)	E_{corr} (V)	$i_{\text{corr}}(\text{Acm}^{-2})$	$b_c(\text{Vdec}^{-1})$	$b_a(\text{Vdec}^{-1})$	$R_p(\Omega/\text{cm}^2)$
Ti_3AlC_2	0	-0.051 ± 0.01	$(40.6 \pm 3) \times 10^{-7}$	0.019	0.015	8.96×10^2
	24	-0.345 ± 0.02	$(101 \pm 5) \times 10^{-7}$	0.019	0.013	3.31×10^2
Ti_2AlC	0	-0.037 ± 0.01	$(1.37 \pm 0.1) \times 10^{-7}$	0.024	0.018	201.13×10^2
	24	-0.325 ± 0.021	$(190 \pm 4.5) \times 10^{-7}$	0.015	0.011	3.34×10^2

Table 2
Electrochemical parameters of MAX phases immersed in HCl

MAX phases	Immersion time (h)	E_{corr} (V)	$i_{\text{corr}}(\text{Acm}^{-2})$	$b_c(\text{Vdec}^{-1})$	$b_a(\text{Vdec}^{-1})$	$R_p(\Omega/\text{cm}^2)$
Ti_3AlC_2	0	-0.419 ± 0.2	$(413 \pm 6) \times 10^{-7}$	0.0380	0.034	1.886×10^2
	24	-0.468 ± 0.1	$(39.6 \pm 1) \times 10^{-7}$	0.0391	0.0362	109.65×10^2
Ti_2AlC	0	-0.145 ± 0.1	$(49.2 \pm 2.1) \times 10^{-7}$	0.046	0.027	15.01×10^2
	24	-0.403 ± 0.1	$(439 \pm 3) \times 10^{-7}$	0.05	0.037	2.103×10^2

Table 3
Electrochemical parameters of MAX phases immersed in HNO_3

MAX phases	Immersion Time (h)	E_{corr} (V)	$i_{\text{corr}}(\text{Acm}^{-2})$	$b_c(\text{Vdec}^{-1})$	b_a (Vdec^{-1})	$R_p(\Omega/\text{cm}^2)$
Ti_3AlC_2	0	-0.538 ± 0.01	$(5.87 \pm 0.1) \times 10^{-7}$	0.0095	0.026	51.46×10^2
	24	-0.417 ± 0.01	$(44.4 \pm 2) \times 10^{-7}$	0.022	0.016	9.30×10^2

Ti_2AlC	0	0.088 \pm 0.01	(90.36 \pm 0.1) $\times 10^{-7}$	0.053	0.042	1125 $\times 10^2$
	24	-0.415 \pm 0.01	(0.058 \pm 0.01) $\times 10^{-7}$	0.009	0.019	4509.89 $\times 10^2$

3.3. Atomic Absorption Spectrometry (AAS)

We have quantified the Ti and Al atoms present in the acid solutions after the potentiodynamic polarization tests with AAS analysis. The results are presented in table 4.

Table 4
AAS analysis results

Acidic solutions	H_2SO_4		HCl		HNO_3	
	Elements dissolved(mg/l)	Ti	Al	Ti	Al	Ti
Ti_2AlC	46.1	264.84	6.12	58.38	13.28	92.54
Ti_3AlC_2	12.3	44.5	3.45	23.1	8.03	35.21

From AAS results we find that the quantities of Al and Ti dissolved in acidic solutions were different for both phases, Al proportion was greater than that of Ti. This means that Al atoms were dissolved first and more intensively than Ti atoms. On the other hand, the proportion of Al dissolved from Ti_2AlC was significantly higher than this dissolved from Ti_3AlC_2 . In fact, the additional Ti atom in Ti_3AlC_2 hinders the rapid dissolution of the Al atoms.

3.4. Surface morphology

The MAX phases (a) Ti_3AlC_2 and (b) Ti_2AlC morphologies before and after the corrosion tests are shown in fig.3.

Before the corrosion, these phases reveal a lamellar morphology with enough porosity as shown in fig. 3 (a) and 3 (b).

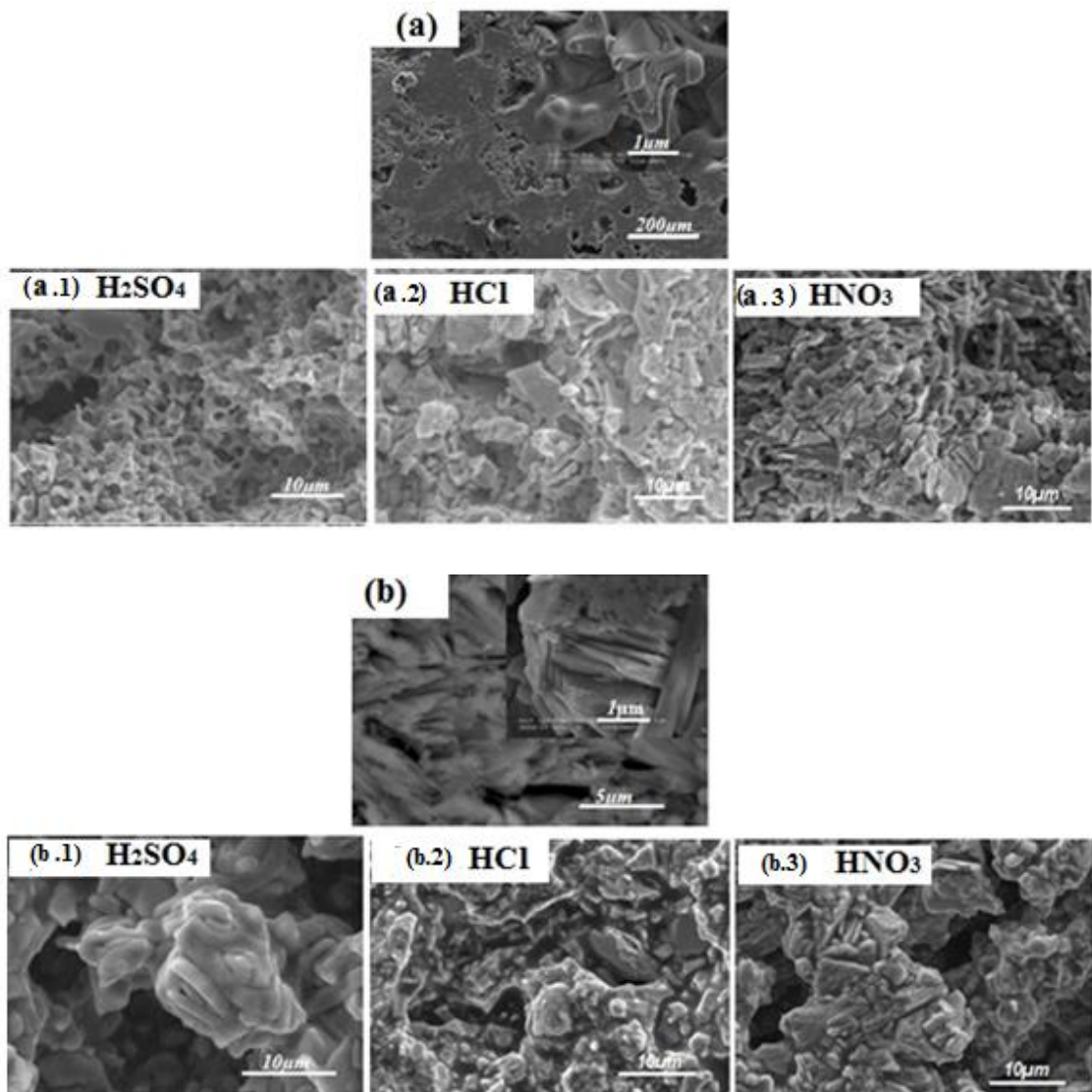


Fig.3. SEM images of Ti_3AlC_2 (a) and Ti_2AlC (b) before and after potentiodynamic polarization tests.

We have seen a serious damage on the Ti_3AlC_2 surface in the tree acid, large cracks caused by material extraction. In H_2SO_4 solution (fig (a.1)) pitting corrosion was more present, and in HCl (fig. (a.2)) and HNO_3 (fig (a.3)) intergranular corrosion and some pitting were observed too.

In three acids solution Ti_2AlC presented a generalized corrosion on the surface of the material, which is due to the rapid formation of protective layer [21].

3.5. Structure analysis

The GAXRD analyzes of Ti_3AlC_2 and Ti_2AlC , before and after corrosion, are shown in Fig. 4. For Ti_3AlC_2 , there is a sharp decrease in the intensity of some diffraction peaks and a complete disappearance of others. This means that an amorphous structure was formed without covering the entire surface and simultaneously with the dissolution of Ti_3AlC_2 . We also observe the broadening of the Ti_3AlC_2 peaks mainly due to the creation of lacunar defects in the crystal lattice.

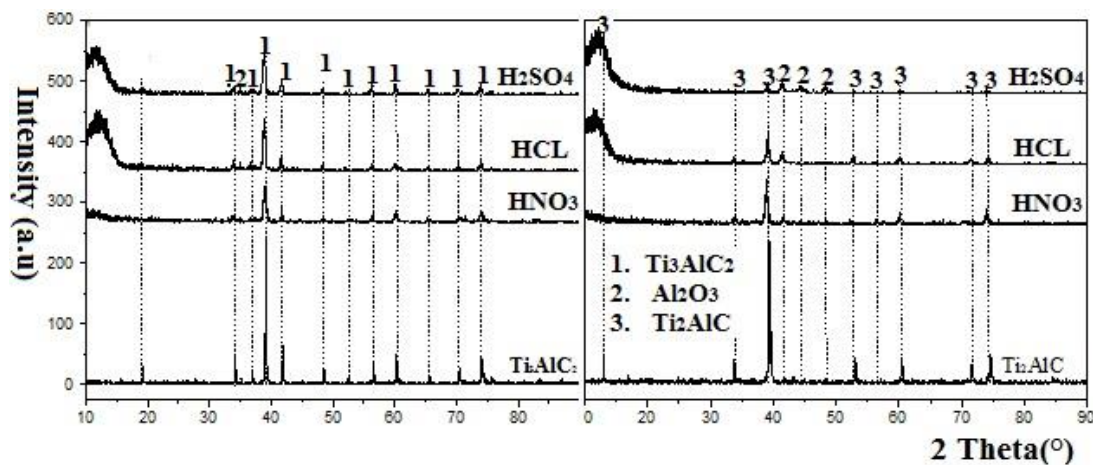


Fig.4. XRD patterns of Ti_3AlC_2 and Ti_2AlC after 24hours of immersion.

On the other hand, the XRD motifs of Ti_2AlC show a complete disappearance of its peaks, which confirms the formation of an amorphous protective film on the immersed surface in the acidic solution. The XRD analysis (Fig. 4) confirms the results obtained from the AAS tests (Table 4). The disappearance of certain peaks of Ti_3AlC_2 and Ti_2AlC after corrosion was confirmed by the AAS analyzes which made it possible to identify and quantify the atoms of Ti and Al dissolved in the acid solutions. XRD analysis of Ti_2AlC revealed the formation of aluminum oxide Al_2O_3 (fig.4) on the surface which justifies a better resistance to corrosion of this compound by the formation of a passivation layer containing alumina.

3.6 Diffusion mechanism proposed

According to the AAS results, the dissolution of Al atoms was greater and faster than that of Ti atoms. This phenomenon promotes the formation of aluminum oxide (Al_2O_3). It can be suggested that the diffusion rate of Al atoms and their position in the lamellar structure of the MAX phase played a very

important role in the dissolution of neighboring Ti atoms, as well as in the corrosion behavior of these phases (Fig. 5).

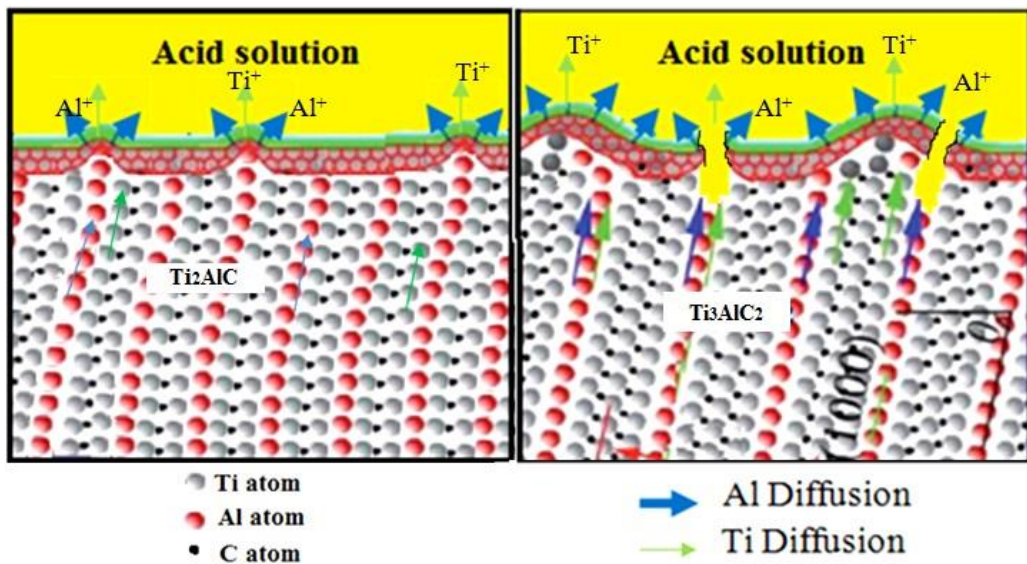


Fig 5. Schematic view of film passivation Ti_3AlC_2 / Ti_2AlC and dissolution of Ti and Al atoms in different acid solutions $\text{H}_2\text{SO}_4/\text{HCl}$ and HNO_3 .

The fact that Ti_3AlC_2 has three layers of Ti alternated by a layer of Al, this compound has a low resistance to corrosion unlike Ti_2AlC . In fact, the Ti atoms slow down the dissolution of the Al atoms, which create a discontinuity in the passivation layer.

4. Conclusions

The corrosion behavior of two MAX phases Ti_3AlC_2 and Ti_2AlC was investigated in H_2SO_4 , HCl and HNO_3 . It was found that Ti_2AlC presented a better passivation and corrosion resistance than Ti_3AlC_2 . We confirm that the lamellar structure of MAX phase favors the diffusion of Aluminum from the structure towards the acidic solution and the number of titanium atoms has a serious impact on the Aluminum dissolution. The existence of three Ti atoms in the hexagonal structure of Ti_3AlC_2 generates obstacles for the dissolution of the Al. It prevents the rapid diffusion of the Al atoms, and consequently leads to discontinuities in the oxide film formed on the material surface. Ti_3AlC_2 has lower corrosion resistance in these acidic solutions. In Ti_2AlC having two Ti atoms, the Al atoms dissolve in greater quantity and form an amorphous protective layer on the surface which gives Ti_2AlC good resistance to corrosion. It has been noted that H_2SO_4

acid is the most aggressive solution compared to the others HCl and HNO_3 . It caused a serious damage to the material surface and a strong pitting corrosion especially for the Ti_3AlC_2 .

R E F E R E N C E S

- [1]. *W. Jeitschko, H. Nowoty, F. Benesovsky. Die H-Phasen, Ti_2TiC , Ti_2PbC , Nb_2InC , Nb_2SnC and $TaGaC$. Monatshefte für Chemie und verwandte Teile anderer Wissenschaften*, **vol. 95**, issue 2, 1964, pp. 431-435.
- [2]. *M.W. Barsoum*, The $M_{n+1}AX_n$ Phases: a new class of solids: thermodynamically stable nanolaminates, *progress in solid state chem.* **vol. 28**, issue 1-4, 2000, pp. 201-281.
- [3]. *D.J. Tallman, B. Anasori, M. W. Barsoum*. A critical review of the oxidation of Ti_2AlC , Ti_3AlC_2 and Cr_2AlC in air, *Materials. Res. Lett.* **vol. 1**, issue 3, 2013, pp. 115-125.
- [4]. *G.M. Song, V. Schnabel, C. Kwakernaak, S. Van der Zwaag, J.M. Schneider, W. G. Sloof*. High temperature oxidation behaviour of Ti_2AlC ceramic at $1200^\circ C$, *Mat at high temp* **vol. 29**, issue 3, 2014, pp. 205-209.
- [5]. *T. Prikhna, S. Dub, A.V. Starostina, M.V. Karpets, T. Cabiosh, P. Chartier*. Mechanical properties of materials based on MAX phases of the Ti-Al-C system, *J. of superhard Mat*, **vol.34**, issue 2, 2012, pp.102-109.
- [6]. *T.C. Duong, A. Talapatra, W. Son, M. Radovic, R. Arróyave*, On the stochastic phase stability of Ti_2AlC - Cr_2AlC , *J. Science reports*, **vol.7**, issue 2017, article number 5138.
- [7]. *L. Cai, Z. Huang, W. Hu, S. Hao, H. Zhai, Y. Zhou*. Fabrication, mechanical properties and tribological behaviors of Ti_2AlC and $Ti_2AlSn_{0.2}C$ solid solutions. *J. of Advanced Ceram*, **vol. 6**, issue 2, 2017, pp. 90-99.
- [8]. *V. Nicolay, N.V. Tzenov, M.W. Barsoum*, Synthesis and characterization of Ti_3AlC_2 , *J. Am. Ceram. Soc.* **Vol. 83**, issue 4, 2000, pp. 825-832.
- [9]. *Y. Mizuno, K. Sato, M. Mrinalini, T.S. Suzuki, Y. Sakka*. Fabrication of textured Ti_3AlC_2 by spark plasma sintering and their anisotropic mechanical properties, *J CeramSoc of Japan*, **vol.121** issue 4, 2013, pp.366-369.
- [10]. *W. Ping, M. Bong-chu, H. Xiao-lin, Z. Wei-bing*. Synthesis of Ti_2AlC by hot pressing and its mechanical and electrical properties, *Tran. Non-ferrous Met. Soc. Chi*, **vol. 17**, issue 2007, pp.1001-1004.
- [11]. *J. Zhu, J. Gao, J. Yang, F. Wang, K. Niihara*. Synthesis and microstructure of layered-ternary Ti_2AlC ceramic by high energy milling and hot pressing, *Mat Sci and Eng A*, **vol. 490**, issue 1-2, 2008, pp. 62-65.
- [12]. *W.B. Zhou, B.C. Mei, J.Q. Zhu, X.L. Hong*. Rapid synthesis of Ti_2AlC by spark plasma sintering technique, *Mat Let*, **vol. 59**, issue 1, 2005, pp. 131-134.
- [13]. *V.I. Vershinnikov, D. Yu. Kovalev*, Synthesis of the Ti_2AlC MAX phase with a reduction step via combustion of a TiO_2 + Mg + Al + C mixture, *Inor. Mat*, **vol. 54**, issue 9, 2018, pp. 949-952.
- [14]. *J. Travaglini, M.W. Barsoum, V. Jovic, T. El-Raghy*. The corrosion behavior of Ti_3SiC_2 in common acids and dilute $NaOH$, *Cor. Sci.* **Vol.45**, issue 6, 2003, pp.1313-1327.
- [15]. *V.D. Jovic, B.M. Jovic, S. Gupta, T. El-Raghy, M.W. Barsoum*. Corrosion behavior of select MAX phases in $NaOH$, HCl and H_2SO_4 , *Cor. Sci.* **vol. 48**, issue 12, 2006, pp. 4274-4228.
- [16]. *X.H. Wang, Y.C. Zhou*. Oxidation behavior of Ti_3AlC_2 at 1000 - $1400^\circ C$ in air. *Cor.Sci*, **vol. 45**, issue 5, 2003, pp.891-907.
- [17]. *D. Sun, A. Zhou, Z. Li, L. Wang*, Corrosion behavior of Ti_3AlC_2 in molten KOH at $700^\circ C$, *J. of Adv. Ceram.* **vol. 2**, issue 4, 2013, pp. 313-317.

- [18]. *D. Li, Y. Liang, X. Liu, Y. Zhou.* Corrosion behavior of Ti_3AlC_2 in $NaOH$ and H_2SO_4 , *J. of the Eur. Ceram. Soc.* **vol.30**, issue 15, 2010, pp. 3227-3234.
- [19]. *J. Fu, T. Fei Zhang, Q. Xia, S-H. Lim, Z. Wan, T-W. Lee, K-H. Kim.* Oxidation and corrosion behavior of nanolaminated MAX-phase Ti_2AlC film synthesized by high-power impulse magnetron sputtering and annealing, *J. Nanomaterials*, **vol.12**, issue 2015, pp. 213-128.
- [20]. *M. Zhu, R. Wang, C. Chen, H. Zhang, G. Zhang.* Electrochemical study on the corrosion behavior of Ti_3SiC_2 in 3.5% $NaCl$ solution, *R. Soc. of Che.* **vol. 7**, issue 21, 2017, pp. 12534-12540.
- [21]. *B.M. Jovic, V.D. Jovic, U.C. Lacnjevac, S.I. Stevanovic, J. Kovac, M. Radovic, N.V. Krstajic.* Ru layers electrodeposited onto highly stable Ti_2AlC substrates as cathodes for hydrogen evolution in sulfuric acid solutions. *J. Electroanalytical Chemistry.* **Vol. 766**, 2016, pp 78-86.